



Task- and domain-specific modulation of functional connectivity in the ventral and dorsal object-processing pathways

Frank E. Garcea^{1,2,6} · Quanjing Chen¹ · Roger Vargas³ · Darren A. Narayan³ · Bradford Z. Mahon^{1,2,4,5}

Received: 21 May 2017 / Accepted: 1 March 2018
© Springer-Verlag GmbH Germany, part of Springer Nature 2018

Abstract

A whole-brain network of regions collectively supports the ability to recognize and use objects—the Tool Processing Network. Little is known about how functional interactions within the Tool Processing Network are modulated in a task-dependent manner. We designed an fMRI experiment in which participants were required to either generate object pantomimes or to carry out a picture matching task over the same images of tools, while holding all aspects of stimulus presentation constant across the tasks. The Tool Processing Network was defined with an independent functional localizer, and functional connectivity within the network was measured during the pantomime and picture matching tasks. Relative to tool picture matching, tool pantomiming led to an increase in functional connectivity between ventral stream regions and left parietal and frontal-motor areas; in contrast, the matching task was associated with an increase in functional connectivity among regions in ventral temporo-occipital cortex, and between ventral temporal regions and the left inferior parietal lobule. Graph-theory analyses over the functional connectivity data indicated that the left premotor cortex and left lateral occipital complex were hub-like (exhibited high betweenness centrality) during tool pantomiming, while ventral stream regions (left medial fusiform gyrus and left posterior middle temporal gyrus) were hub-like during the picture matching task. These results demonstrate task-specific modulation of functional interactions among a common set of regions, and indicate dynamic coupling of anatomically remote regions in task-dependent manner.

Keywords Functional MRI · Functional connectivity · Manipulable objects · Dorsal stream · Ventral stream · Tool pantomiming · Tool identification

Electronic supplementary material The online version of this article (<https://doi.org/10.1007/s00429-018-1641-1>) contains supplementary material, which is available to authorized users.

✉ Bradford Z. Mahon
mahon@rcbi.rochester.edu

¹ Department of Brain and Cognitive Sciences, Meliora Hall, University of Rochester, Rochester, NY 14627-0268, USA

² Center for Visual Science, University of Rochester, Rochester, USA

³ School of Mathematical Sciences, Rochester Institute of Technology, Rochester, USA

⁴ Department of Neurosurgery, University of Rochester Medical Center, Rochester, USA

⁵ Department of Neurology, University of Rochester Medical Center, Rochester, USA

⁶ Moss Rehabilitation Research Institute, Elkins Park, PA, USA

Introduction

The ability to identify, grasp, and manipulate objects in a functionally appropriate manner requires the integration of computations that are anatomically segregated in distinct brain regions. Early functional neuroimaging research identified regions within the ventral object-processing pathway that exhibit category preferences for small manipulable objects, including the medial aspect of the fusiform gyrus bilaterally, and the left posterior middle/inferior temporal gyrus (e.g., Chao et al. 1999). Subsequent studies identified category preferences for manipulable objects in the left anterior inferior parietal lobule (supramarginal gyrus), left posterior parietal cortex, and in ventral and dorsal premotor cortex (e.g., see Chao and Martin 2000; Culham et al. 2003; Grafton et al. 1997; Mahon et al. 2007; for review, see; Lewis 2006). We refer to this set of regions as the Tool Processing Network to capture the broad observation that

recognizing and physically interacting with objects involves coordinated processing across this network.

Different regions within the Tool Processing Network are hypothesized to carry out different aspects of tool recognition and use. Regions within ventral temporo-occipital cortex represent visual surface and texture properties (e.g., Cant and Goodale 2007, 2011; Miceli et al. 2001; Simmons et al. 2007; Stassenko et al. 2014). The left posterior middle temporal gyrus (sometimes inferior temporal gyrus) is sensitive to mechanical motion of manipulable objects (e.g., see Beauchamp et al. 2002, 2003) and likely processes action-relevant semantic information related to objects generally, and manipulable objects specifically (e.g., see Bedny et al. 2008, 2012; Buxbaum et al. 2014; Kable et al. 2002; Kemmerer et al. 2008; Mahon et al. 2007; Peelen et al. 2012; Tranel et al. 1997, 2003; for discussion, see; Bedny and Caramazza 2011; Martin 2007). The left ventral (e.g., see Chao and Martin 2000) and dorsal premotor cortex (e.g., Grafton et al. 1997) are involved in action planning and sequencing.

The left dorsal occipital cortex, extending into posterior parietal cortex, processes volumetric and spatial information relevant for reaching to objects in peripersonal space (e.g., see Cavina-Pratesi et al. 2007; Culham et al. 2003; Fang and He 2005; Galletti et al. 1993; Gallivan et al. 2015; Konen et al. 2013). Recent evidence suggests that posterior parietal regions contribute to processing of three-dimensional structure and shape (e.g., see Freud et al. 2017b; Van Dromme et al. 2016; see also Konen and Kastner 2008). The left supramarginal gyrus in the inferior parietal lobule processes complex object-associated manipulation knowledge, and the adjacent anterior IPS supports hand shaping for object-directed grasping (e.g., see Brandi et al. 2014; Binkofski et al. 1998; Chen et al. 2016; Frey et al. 2005; Konen et al. 2013; Moll et al. 2000; Peeters et al. 2013; Rumiati et al. 2004; Valyear et al. 2007; for review, see; Buxbaum and Binkofski 2013; Buxbaum 2017; Freud et al. 2016; Ishibashi et al. 2016; Kastner et al. 2017; Orban and Caruana 2014), and is engaged when participants explicitly retrieve manipulation knowledge associated with manipulable objects (e.g., see Boronat et al. 2005; Canessa et al. 2008; Chen et al. 2016, 2017b; Gallivan et al. 2013; Kellenbach et al. 2003).

A great deal of what we know about the Tool Processing Network comes from patient studies, indicating that it is possible to selectively impair specific processes within the broader tasks of recognizing and using objects. For instance, since the time of Liepmann (1905), it has been known that lesions to the supramarginal gyrus can cause impairments for object manipulation (i.e., limb apraxia; see Liepmann 1905; see also; Ochipa et al. 1989; Buxbaum et al. 2000; Negri et al. 2007; Garcea et al. 2013; Salazar-López et al. 2016; for reviews, see; Rothi et al. 1991; Cubelli et al. 2000; Johnson-Frey 2004; Mahon and Caramazza 2005; Goldenberg 2009; Binkofski and Buxbaum 2013). In contrast, lesions to

the superior and/or posterior parietal lobule typically leave object manipulation intact but can affect object-directed reaching and/or grasping (and reaching and grasping can be separately impaired by focal lesions; e.g., see Pisella et al. 2006, 2000; for review, see; Milner and Goodale 2008; Rossetti et al. 2003). Within the ventral stream, focal lesions can impair visual object recognition (Goodale et al. 1991), or knowledge of surface properties (Cavina-Pratesi et al. 2009, 2010; Miceli et al. 2001; Stassenko et al. 2014), or can differentially affect visual recognition of small manipulable objects (Bruffaerts et al. 2014).

A growing number of studies have measured functional interactions among regions within the Tool Processing Network during task-based fMRI (e.g., see Almeida et al. 2013; Chen et al. 2017a; Gallivan et al. 2013; Garcea and Mahon 2014; Hutchison and Gallivan 2018; Mahon et al. 2007, 2013; Noppeney et al. 2006; Vingerhoets and Clauwaert 2015). Recently, we (Garcea and Mahon 2014) showed that tool-responsive voxels within the left parietal lobule could be parcellated on the basis of their differential functional connectivity to other regions of Tool Processing Network, including frontal-motor areas (left ventral premotor cortex), the ventral and lateral temporal areas (left medial fusiform gyrus; left posterior middle/inferior temporal gyrus), and the dorsal visual pathway (left dorsal occipital cortex). In addition, recently, Stevens et al. (2015) found that the left medial fusiform gyrus expressed privileged functional connectivity with the left inferior parietal lobule and left ventral premotor cortex at rest (see also Chen et al. 2017a; Hutchison et al. 2014; Peelen et al. 2013; for convergent findings with task-based data, see; Almeida et al. 2013; Garcea and Mahon 2014; Mahon et al. 2007, 2013).

In summary, there is a relatively rich understanding of the broad computations that are carried out by regions within the Tool Processing Network, and a solid foundation of empirical work that has elucidated functional interactions across the network. However, studies to date have not systematically varied task demands to evaluate how functional coupling among regions of the Tool Processing Network may be modulated. Understanding how functional interactions across the Tool Processing Network change as a function of task demands is a critical first step toward understanding how processing across multiple regions is integrated in the service of a behavioral goal. Here, we hold visual stimulation constant, and isolate the effects of task-dependent modulations of functional connectivity over and above baseline levels of functional coupling. In subsequent analyses, we use a graph theoretic metric, betweenness centrality, to measure the centrality (or “hubness”) of each region (vertex) in each task, and of each connection (edge) in each task.

Participants were asked to visually match images of tools or to pantomime the use of those tools during fMRI scanning. Animal stimuli were included in the matching and

pantomiming conditions (e.g., gesture petting a rabbit) to serve as a baseline with which to determine whether modulation of functional connectivity for manipulable object stimuli was specific to those stimuli (and task) or rather modulated only by task, regardless of the target of the action. We acknowledge, up front, that there are many differences between gesturing ‘petting a rabbit’ and gesturing ‘using scissors,’ including that the former is an intransitive action, while the latter is transitive, and the former is more or less the same for different small cuddly animals (e.g., cat and rabbit), while actions can be quite different for tools. Nonetheless, the contribution of that control is to ask whether patterns of functional coupling observed for tools are observed for any cued manual actions.

To be able to study functional connectivity specific to each stimulus and task, a sparse event-related design was employed in which 40 s was interposed between critical stimuli in the experiment. During the 40-s interstimulus periods, phase-shifted images of the target stimuli were presented at the same alternation rate as during the critical stimulus blocks. This design was used, such that low-level visual stimulation remained constant throughout the experimental run, and thus, any changes in network connectivity elicited by the onset of stimuli (in the context of a given task) could be specifically related to the object as opposed to general visual stimulation.

We predicted that pantomiming tool use would elicit increased functional connectivity among ventral stream regions and regions in left parietal cortex. This is because high-level visual and semantic information about the stimulus represented in the ventral object-processing pathway is necessary to access object-directed action knowledge in the left inferior parietal lobule (e.g., see Almeida et al. 2013; Garcea et al. 2016; Kristensen et al. 2016; Mahon et al. 2013). In contrast, we predict that functional connectivity during picture matching would increase among regions that process high-level visual and semantic information within the ventral object-processing pathway.

Methods

Participants

Twelve University of Rochester Undergraduate students (9 females; mean age = 20 years, SD = 1.13 years) participated in the experiments (total of 31 scan sessions) in exchange for payment. All participants were right-handed, as assessed with the Edinburgh Handedness Questionnaire. They had normal or corrected to normal vision, were native English speakers, and had no history of neurological disorders. All participants gave written informed consent in accordance

with the University of Rochester Research Subjects Review Board.

General procedure

Stimulus presentation was controlled with ‘A Simple Framework’ (ASF; Schwarzbach 2011) written in MATLAB using the Psychophysics Toolbox (Pelli 1997), or E-Prime Professional Software 2.0 (Psychology Software Tools, Inc., Sharpsburg, PA, USA). All participants viewed the stimuli binocularly through a mirror attached to the head coil adjusted to allow foveal viewing of a back-projected monitor (temporal resolution = 120 Hz). Each participant took part in the first scanning session, which began with (a) a 6-min T1 anatomical scan, and (b) 8 7-min runs of the tool pantomiming and n-back picture matching experiment. Two additional localizer sessions followed; 10 of the 12 participants took part in the first localizer session, and 9 of those 10 individuals took part in the second localizer session. The first localizer scan consisted of 6 3-min runs of an object-responsive category localizer experiment (see below for experimental details); the remainder of this session was dedicated to an experiment that was not germane to the current investigation and not analyzed herein (a study investigating MT/V5). The second localizer session consisted of (a) 2 8-min runs of a motor cortex localizer experiment; (b) 2 8-min runs of a somatosensory cortex localizer (data not analyzed herein); (c) 2 6-min runs of resting state fMRI (data not analyzed herein); and (d) a 15-min diffusion tensor imaging (DTI) scan (data not analyzed herein).

Tool pantomiming and n-back picture matching

Design

Each participant completed four runs of the tool pantomiming and four runs of the n-back picture matching experiment (hereafter, ‘picture matching’ experiment); both tasks were blocked by run (189 volumes per run, below for further details). All aspects of stimulus presentation were identical across the two tasks. Participants were presented with 8-s miniblocks in which 8 different exemplars of an object were presented (i.e., 8 different screwdrivers were presented in one miniblock). Each image was presented for 500 ms, and was followed by a centrally-presented fixation cross (presented for 500 ms). Miniblocks were interspersed by 40-s baseline periods, in which phase-shifted versions of the ‘intact’ stimuli were presented; the scrambled stimuli were flickering at the same frequency (i.e., 500 ms of stimulus followed by 500 ms of fixation), and were presented in the same physical location, as the intact stimuli. In this way, the initial BOLD response to the onset of a miniblock of stimuli would not be driven by low-level visual information

but rather by the high-level object-relevant information that is the focus of the study. During the portions of the experiment in which scrambled images were presented, participants were instructed to pay attention to the stimuli, and to prepare for the next event in which a ‘real’ stimulus would be presented. Each experimental run began and ended with 16 s of fixation.

There were 8 items used in the experiment, with 8 exemplars of each item (i.e., 8 different pictures of screwdrivers were chosen for the item ‘screwdriver, for a total of 64 total items); 6 items were manipulable objects (scissors; pliers; knife; corkscrew; bottle opener; screwdriver—see Chen et al. 2016, 2017b; for material selection) and 2 were animals (cat; rabbit). Before the experiment proper, all participants were presented with the 64 items, and were instructed as to how to pantomime tool use (for precedent on this task, see Chen et al. 2016). For animals, participants were shown how to pantomime petting the animal while in the scanner (as if it were sitting on their lap).

Procedure

In the pantomiming experiment, the participants were cued to pantomime object use when the images of objects were presented; successful pantomiming involved a pantomimed grasp of the object, and movement of the hands and wrist, as if the participant were holding and using the object. Participants were specifically instructed to not move their forearm and upper arm. In the picture matching experiment, the participants were instructed to pay attention to the items, and to hit a button with their right index finger if any of the images within the 8-s miniblock repeated. An analysis of performance during the picture matching task indicated that while participants were accurate in detecting repeats (mean hit rate = 87%; standard error of the mean across participants, 3%), participants tended to have high rates of false alarm (mean false alarm rate = 54%; standard error of the mean across participants = 4%), resulting in a modest d' (mean d' = 0.96, SEM across participants = 0.19; one-sample t test: $t(11) = 5.15$, $p < 0.001$). This modest d' is due to the fact that this was a difficult n-back matching task, involving tracking repeats across 8 briefly presented images of different exemplars of a given object type; nonetheless, these behavioral data indicate that participants were attending to the images presented and performing the matching task.

The pantomiming and picture matching tasks were counterbalanced in an ABAB/BABA manner across runs and across participants evenly. For example, the first run that the first participant completed was pantomiming, and the second run was picture matching; in contrast, the first run that the second participant completed was picture matching, and the second run was pantomiming. Within a given run, each exemplar was presented once (except for intermittent

repeats within a block); within each miniblock, exemplar order was random.

A permanently installed camera in the same room as the MRI had the participants hand and lower body in view; that camera feed was fed in real time to the MR control room. In this way, the experimenters were able to monitor each participant’s pantomiming performance in real time. The participants were informed and corrected immediately if there were any issues with respect to executing object pantomimes or animal petting movements. This setup also allowed the experimenters to verify that participants were producing movements accurately during the primary motor cortex localizer (see below).

Tool- and object-responsive localizer experiment

Design and procedure

To localize object-responsive areas in the brain, including tool-preferring regions, participants viewed scrambled and intact images of tools, animals, famous faces, and famous places (for prior use of this localizer, see Chen et al. 2016, 2017a, b; Fintzi and Mahon 2014). Twelve grayscale photographs of tools, animals, faces, and places were used; there were eight exemplars of each (i.e., eight different hammers; eight different pictures of Bill Clinton). This resulted in a total of 96 images per category, and 384 total images. Phase-shifted versions of the stimuli were created to serve as a baseline condition. Participants viewed the images in a miniblock design. Within each 6-s miniblock, 12 stimuli from the same category were presented for 500 ms each (0-ms interstimulus interval), and 6-s fixation periods were presented between miniblocks. Within each run, eight miniblocks of intact images and four miniblocks of phase-shifted versions of the stimuli were presented with the constraint that a category of objects did not repeat across two successive miniblocks. All participants completed six runs of the category-localizer experiment (91 volumes per run).

Primary motor cortex localizer

Design and procedure

This localizer was designed to identify the primary motor representation of the hand and wrist. Participants were instructed to rotate or flex their left or right hand or foot upon presentation of a visual cue. While participants were lying supine in the scanner, a black screen with the words, for instance, “LF Rotate”, in a white font was visually presented, and the participant then rotated their left foot at the ankle. Eight actions (left/right × hand/foot × rotate/flex) were presented in miniblocks of 12 s, interspersed by 12-s fixation periods. Each action was presented twice per run,

with the constraint that an action did not repeat across two successive miniblock presentations. During flexion trials, the participants were instructed to bring their hands or feet from a resting, inferior position, upwards, into an extended position, and then to smoothly return their hand or foot back (~ 0.5 oscillation per second). Similarly, during the rotation miniblocks, the participants were instructed to rotate their hands or feet at the wrist or ankle, while minimizing elbow and hip movements (respectively, ~ 0.5 oscillation per second). Participants were given explicit directions and practice with the cues before entering the scanner. Because the participants were lying supine in the scanner, all actions were performed out of their view. Participants completed two runs of the primary motor cortex localizer experiment (210 volumes per run).

MR acquisition and analysis

MRI parameters

Whole-brain BOLD imaging was conducted on a 3-Tesla Siemens MAGNETOM Trio scanner with a 32-channel head coil located at the Rochester Center for Brain Imaging. High-resolution structural T1 contrast images were acquired using a magnetization prepared rapid gradient echo (MP-RAGE) pulse sequence at the start of each participant's first scanning session (TR = 2530, TE = 3.44 ms, flip angle = 7 degrees, FOV = 256 mm, matrix = 256×256 , $1 \times 1 \times 1$ mm sagittal left-to-right slices). An echo-planar imaging pulse sequence was used for T2* contrast (TR = 2200 ms, TE = 30 ms, flip angle = 90° , FOV = 256×256 mm, matrix = 64×64 , 33 sagittal left-to-right slices, voxel size = $4 \times 4 \times 4$ mm). The first six volumes of each run were discarded to allow for signal equilibration (four volumes at image acquisition and two at preprocessing).

Acquisition of physiological variables

We collected heart rate and respiration time-series aligned with the acquisition of functional data during the pantomiming and picture matching experiment (as well as during all other functional MRI scans). All physiological recordings were acquired by Siemens software on the console computer, and saved for offline analysis. Heartbeats were measured with a finger photoplethysmographic (PPG) reader, which measures heart rate by examining the reflectance of light from a light-emitting diode off the skin onto a photodiode in the PPG reader. Respiration was recorded with a pneumatic belt placed around the upper abdomen of each participant. Both of these physiological measures were regressed from the BOLD signal prior to computing functional connectivity (along with the variance in the BOLD signal due to motion, as detailed below); all functional connectivity analyses were

carried out over the residual BOLD time-series data having regressed those sources of noise (e.g., see Gotts et al. 2013a, b; Saad et al. 2013). In additional analyses reported in the Supplemental Online Materials (see below for details), we demonstrate that the core findings were present when also regressing the global mean time course.

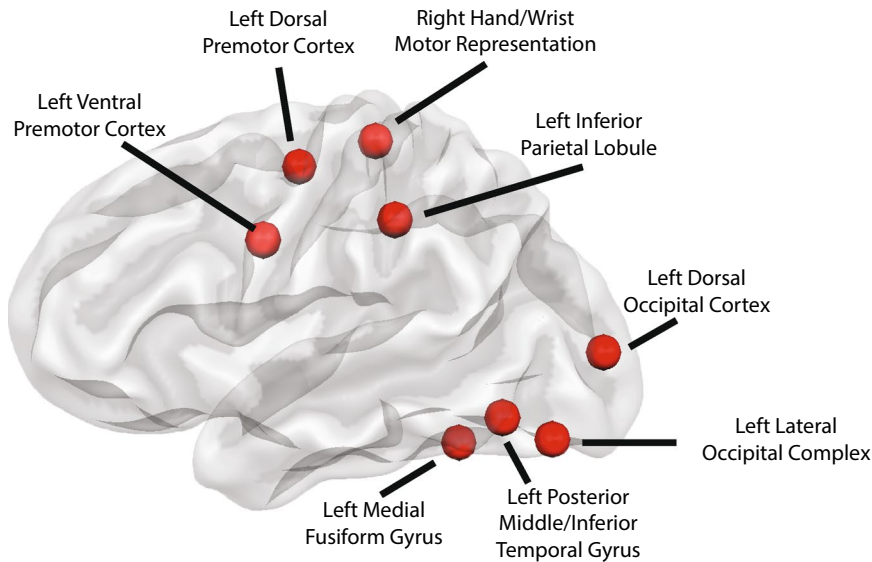
fMRI data analysis

fMRI data were analyzed with the BrainVoyager software package (Version 2.8.2) and in-house scripts drawing on the BVQX toolbox written in MATLAB. Preprocessing of the functional data included, in the following order, slice scan time correction (since interpolation), 3D motion correction with respect to the first volume of the first functional run, and linear trend removal in the temporal domain (cutoff: two cycles within the run). Functional data were registered (after contrast inversion of the first volume) to high-resolution deskulled anatomy on a participant-by-participant basis in native space. For each participant, echo-planar and anatomical volumes were transformed into standardized space (Talairach and Tournoux 1988). All functional data were smoothed at 6 mm FWHM (1.5 mm voxels) and interpolated to 3 mm^3 . For all experiments, the general linear model was used to fit beta estimates to the experimental events of interest. Experimental events were convolved with a standard 2-gamma hemodynamic response function. The first derivatives of 3D motion correction from each run were added to all models as regressors of no interest to attract variance attributable to head movement.

ROI definition

We localized eight ROIs at the single-subject level in the nine individuals who took part in the functional localizer tasks. To ensure that the time-series from each ROI for each subject was generated from the same number of voxels, we created spherical seed regions (6-mm diameter) centered on the peak voxel for each ROI. Six of the eight ROIs were defined using the tool stimuli in the object localizer task; the primary motor representation of the right hand/wrist was defined with the motor localizer task; the left lateral occipital complex was defined using the object localizer task (intact images > scrambled images). Because 3 of the 12 participants did not take part in the localizer scanning sessions, we used group-level general linear models (random effects analysis, $n = 9$) to define ROIs for those three participants' functional connectivity analyses (based on the other nine participants who did complete the functional localizer). Figure 1a plots spherical ROIs centered on the group-level peak voxel (see Table 1 for the peak coordinates).

A Functionally localized Regions of Interest in the Tool Processing Network



B Schematic of the approach for computing stimulus- and task-driven functional connectivity

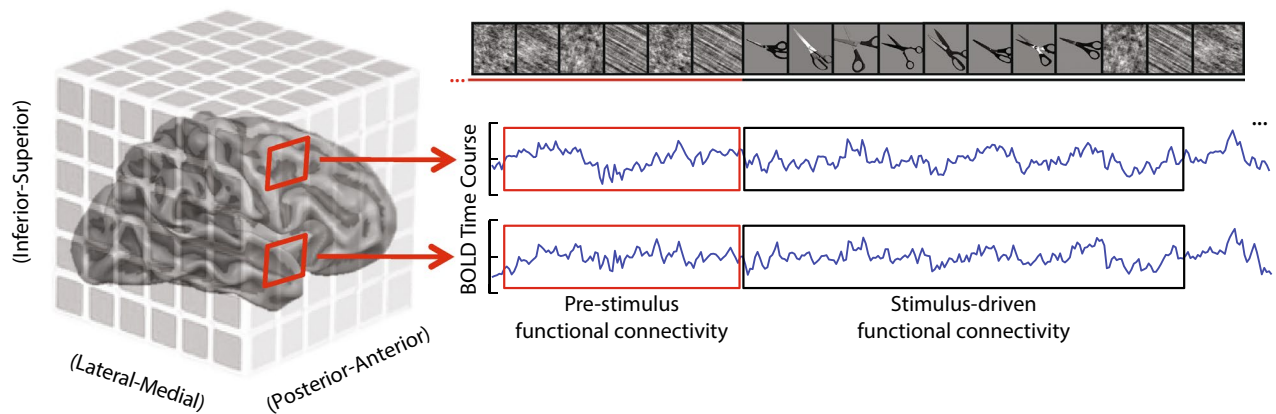


Fig. 1 Overview of the Tool Processing Network and analytic approach. Spheres centered on the peak voxel from the functional localizer, determined on a participant-by-participant basis, served as regions of interest (ROIs). **a** Results from the functional localizer scans are recast as spheres, 6 mm in diameter, centered on the peak voxel from the respective functional localizer scans (using group

defined peaks for visualization). **b** Schematic of computing functional connectivity between two ROIs, in which functional connectivity was computed over portions of the BOLD time course data associated with phase-shifted stimuli (i.e., prestimulus functional connectivity), or over data corresponding to stimulus presentation (i.e., stimulus-driven functional connectivity)

Definition of tool-preferring regions

Tool-preferring regions were identified with the whole-brain contrast of Tools > Animals. If Tools > Animals did not elicit differential BOLD contrast in a region of the Tool Processing Network in a particular subject, then the contrast of Tools > (Animals + Faces + Places, weighted equally) was used to define tool preferences. We first sought to identify regions at the FDR-corrected level of $q < 0.05$; if no voxels in a region survived at the single-subject level, the threshold was relaxed (to a maximum of $p < 0.05$, uncorrected). There is little concern here with false positives (e.g.,

from using a $p < 0.05$ threshold) as the definition of ROIs is highly constrained by the prior literature (e.g., Chao et al. 1999; Chao and Martin 2000; Grafton et al. 1997; Noppeney et al. 2006), including studies in our group using the same localizer (Almeida et al. 2013; Chen et al. 2016, 2017a, b; Erdogan et al. 2016; Garcea et al. 2016, 2017; Garcea and Mahon 2014; Kristensen et al. 2016; Mahon et al. 2013) and because the analyses reported below used those ROIs to compute functional connectivity over independent data. In this way, we defined tool-preferring ROIs in the left inferior parietal lobule, left dorsal premotor cortex, left ventral premotor cortex, left posterior middle/inferior temporal

Table 1 Talairach coordinates for peak voxels from regions showing differential BOLD contrast for Tool stimuli, Objects, and the Right Hand/Wrist Motor Area

Region	Mean peak voxel coordinate (XYZ)			Standard deviation across subjects (mm)		
Tools areas (tools > animals)						
Left dorsal premotor cortex	-25	-11	52	8.9	6.8	5.4
Left ventral premotor cortex	-45	-3	32	9.8	4.6	10
Left inferior parietal lobule	-45	-35	37	10.5	7	5.5
Left medial fusiform gyrus	-32	-50	-14	4.6	7.9	4
Left posterior middle/inferior temporal gyrus	-43	-59	-8	4	6.3	6.4
Left dorsal occipital cortex	-31	-88	7	3.9	5.4	6.9
Object recognition areas (intact images > scrambled images)						
Left lateral occipital cortex	-41	-71	-13	4.2	9	5.7
Right hand/wrist motor area (right hand movements > right foot movements)						
Right hand/wrist motor cortex	-32	-30	56	4.2	6.2	5.6

gyrus, left medial fusiform gyrus, and in left dorsal occipital cortex. The peak voxel coordinates (average \pm standard deviation across subjects) are listed in Table 1. Note that we did not define the right medial fusiform gyrus or the right lateral occipital cortex, because the other left hemisphere ROIs did not have right hemisphere homologues. This consideration is particularly important for the graph theoretic analyses that compute global measures of network structure, and which would be affected by including right hemisphere homologues for only two of the left hemisphere ROIs.

Definition of left lateral occipital cortex

The lateral occipital cortex ROI was defined using the category-localizer experiment and the whole-brain contrast of Intact Objects > Scrambled Objects (i.e., collapsing across all categories). This contrast yielded differential BOLD contrast for intact objects bilaterally in lateral occipital complex (e.g., see Grill-Spector et al. 1998; Malach et al. 1995); for the purpose of the current study, we focus on the left lateral occipital complex for functional connectivity analyses.

Definition of primary motor representations for the right hand/wrist

The right hand/wrist motor representation was identified with the whole-brain contrast of right hand movements > right foot movements. This contrast identified a dorsal-lateral region of the precentral gyrus in good agreement with the location of the primary motor representation of the right hand/wrist.

Ensuring rigor and replicability of core findings

Given recent discussion in the literature about experimental power and replicability (e.g., see Eklund et al. 2016), and

that we had a sample size of 12, we took specific steps to ensure all findings are statistically robust. To that end, we conducted a split-half analysis. We analyzed functional connectivity modulations on three groupings of the data: all data (4 runs per task), and separately for data from even runs (runs 2 and 4) and odd runs (runs 1 and 3). Below, we report that an edge exhibits significant functional connectivity only if the observed effect meets the strict criteria of surviving FDR $q < 0.05$ across three analyses: (1) all four runs, (2) odd runs, and (3) even runs.

Functional connectivity analyses

Several sources of noise were regressed out of the time-series data (after the preprocessing steps described above): (1) the change in head position across volumes, (2) the time-series of heart beats across volumes, and (3) the time-series of respiration across volumes. All functional connectivity analyses were conducted over the residuals of that regression model. Recent work has raised concerns with the procedure of regressing the global mean time course prior to computing functional connectivity (e.g., see Gotts et al. 2013a, b; Saad et al. 2013). For that reason, the core analyses are reported below without regressing the global mean time-series. We also re-run all functional connectivity analyses reported herein after regressing the global mean. Almost all of the core findings observed when global mean was not regressed are also present when regressing the global mean; in addition, there are some edges that emerge as significant when regressing global mean which were not significant when global mean was not regressed. We focus our interpretation that are observed to be significant at robust thresholds (FDR $q < 0.05$, as described above) across both analyses (i.e., not regressing and regressing global mean). Below, we report all analyses over data without global mean regression, and in the Supplemental Online Materials, we

report parallel analyses having regressed global mean (e.g., see Supplemental Tables 1, 2, and 3).

To measure task-based modulation of functional connectivity, we extracted the BOLD time-series data that corresponded to miniblock events, and separately, the portions of the BOLD time-series immediately preceding each miniblock in which phase-shifted images were presented. We began by extracting 26.4 s (12 volumes) of time-series data aligned to the onset of each miniblock. The first 8 s of that time-series were associated with stimulus presentation and task execution (pantomiming or picture matching) and the remaining 18.4 s corresponded to phase-shifted image stimulation that immediately followed stimulus presentation. Because there were 8 miniblocks of intact stimuli presented in each run, for each run, we derived eight 12-volume-long time-series segments.

To derive a measurement of prestimulus functional connectivity, we extracted the 26.4 s (12 volumes) of time-series data that immediately preceded the onset of the miniblocks. There were not 12 volumes of phase-shifted images preceding the first miniblock in each run; thus, 7 prestimulus (12-volume-long) time-series segments were extracted for each run, and an eighth “prestimulus” time-series segment was extracted from the 12 volumes that followed the eighth miniblock event (i.e., that would have immediately preceded a 9th miniblock of images, had there been a 9th miniblock). As noted above, there were 40 s of phase-shifted stimulus presentation between miniblocks; therefore, there was an overlap of 2 volumes (4.4 s) between the tail-end of time-series segments corresponding to miniblock epochs, and the front-end of time-series corresponding to prestimulus epochs (see Fig. 1b for a schematic of the functional connectivity analysis). If anything, this overlap works against observing a dissociation in functional connectivity as a function of the onset of the stimulus compared to the prestimulus epoch.

Separate stimulus-driven and prestimulus time-series matrices (row volumes, column ROIs) were created for each time-window that was analyzed, and the matrices for tools and animals were separated (for stimulus-driven and prestimulus conditions). There were, therefore, six matrices for each run corresponding to tool stimuli, and six matrices for pretool epochs from each run; there were two matrices for each run for animal miniblocks and two matrices for preanimal epochs. Each pairwise combinations of ROIs within the time-series matrix were correlated, and the resulting correlation matrices were averaged together within category, separately for the prestimulus and stimulus-driven conditions.

This resulted in 8 averaged 8×8 arrays (8 ROIs \times 8 ROIs) for each of the 12 participants (96 total correlation matrices): the 8 matrices for each participant reflected the 8 cells of the design: Stimulus Category (two levels: tools, animals) \times Task (two levels: pantomime, picture matching) \times Epoch (two levels: prestimulus, stimulus-driven). Subject-level correlation

matrices were Fisher-transformed; paired *t* tests were used to evaluate whether and how functional connectivity was modulated as a function of task and category, over and above the prestimulus condition. To control for multiple comparisons associated with the large number of *t* tests performed, all *t* scores were corrected for false discovery rate (FDR) at $q < 0.05$; *t* values that did not survive the FDR threshold were not interpreted and those edges were excluded from additional analyses (e.g., betweenness centrality).

Betweenness centrality analyses

The graph theoretic measure of betweenness centrality was used to succinctly capture the degree to which a given region (vertex), or a given connection (edge), exhibited increased centrality to network connectivity during the tool pantomiming and tool picture matching tasks. Betweenness centrality was computed using a toolbox written for Matlab (Gleich 2006). Betweenness centrality is a metric that quantifies, among all of the paths in a network between each unique pair of vertices, the number of paths that pass through a given vertex (i.e., vertex centrality) or edge (i.e., edge centrality; see e.g., Brandes et al. 2015; Freeman 1977; Freeman et al. 1991). In neural network analysis, vertices that express strong betweenness centrality are thought to connect (anatomically or functionally) disparate portions of a network (see, e.g., Rubinov and Sporns 2010).

We started with each participant's 8×8 (i.e., 8 ROIs) functional connectivity matrix (not Fisher-transformed) associated with tool pantomiming and tool picture matching. Each subject's functional connectivity matrix was then masked based on the group-level (FDR $q < 0.05$) results comparing stimulus-driven connectivity to the prestimulus baseline epoch (see Tables 2, 3), such that only edges that were significant at the group-level went into the single-subject computation of betweenness centrality. Note that, akin to the functional connectivity analyses, the mask used to remove non-significant data met the strict criteria that edges survived FDR-corrected alpha levels when using (1) all runs of data, (2) odd runs, and (3) even runs. Next, we converted measures of functional connectivity (correlation coefficients) into dissimilarity values by subtracting each edge correlation value from 1; this ensured that larger functional connectivity values were represented as smaller dissimilarity values. We then computed the betweenness centrality of vertices and edges for each subject-level dissimilarity matrix, separately for tool pantomiming and tool picture matching, and averaged the subject-level betweenness centrality results to obtain a group-level betweenness centrality measure for each vertex and each edge. Note that statistics were not performed on the resulting graphs, because only data that survived strict thresholds went into the computation of betweenness centrality to begin with.

Table 2 *T* matrix for the interaction between task (pantomiming > picture matching) and epoch (stimulus-driven functional connectivity > prestimulus functional connectivity)

	PMd	PMv	LIPL	LMFG	LMTG	LDO	RHWM	LLOC
PMd	–							
PMv	–	–						
LIPL	–	–	–					
LMFG	–	–	–	–				
LMTG	–	–	–	–5.21 (11)	–			
LDO	–	–	–	–4.57 (12)	–	–		
RHWM	4.16 (11)	–	4.72 (12)	3.51 (10)	9.29 (12)	3.80 (11)	–	
LLOC	–	–	–	–6.15 (12)	–	–4.42 (11)	5.35 (12)	–

Edges are reported that meet the criteria of surviving FDR $q < 0.05$ when tested over all runs of data, and even and odd runs alone (split-half analysis). Positive t values indicate a relative increase in functional connectivity during pantomiming, while negative t values indicate a relative increase in functional connectivity during object picture matching. In parentheses, we list the number of participants whose data are consistent with the direction of the interaction effect

PMd left dorsal premotor cortex, *PMv* left ventral premotor cortex, *LIPL* left inferior parietal lobule, *LMFG* left medial fusiform gyrus, *LMTG* left posterior middle/inferior temporal gyrus, *LDO* left dorsal occipital cortex, *RHWM* right hand/wrist motor representation, *LLOC* left lateral occipital cortex

Results

There were three factors in our design and analysis: Task (2 levels; pantomiming, picture matching), Epoch (2 levels; stimulus-driven functional connectivity, prestimulus functional connectivity), and Category (2 levels: tools, animals). We first tested directional interactions between Task and Epoch to understand how functional connectivity was differentially modulated by tool pantomiming and tool picture matching, compared to the prestimulus baseline (i.e., “[Tool_{Pantomiming} – Pre-Tool_{Pantomiming}] – [Tool_{Picture matching} – Pre-Tool_{Picture matching}]” and “[Tool_{Picture matching} – Pre-Tool_{Picture matching}] – [Tool_{Pantomiming} – Pre-Tool_{Pantomiming}]”). We then analyzed the degree to which functional connectivity was modulated by the factor Epoch, separately for tool pantomiming and tool picture matching (equivalent to performing paired t tests). Analogous analyses are carried out for the data with animal stimuli to test whether modulations of functional connectivity observed for tool stimuli generalize to another, non-tool, visual stimulus.

Interaction between Task (pantomiming, picture matching) and Epoch (prestimulus, stimulus-driven) for tool stimuli

We first sought to measure which edges exhibited functional connectivity modulated by the interaction between Task (pantomiming vs. picture matching) and Epoch (stimulus-driven functional connectivity vs. prestimulus functional connectivity). The resulting edge modulations are plotted in Fig. 2a, and the t scores are listed in Table 2 (see also Fig. 2a.ii). Relative to tool picture matching, functional connectivity during tool pantomiming increased among fronto-parietal motor structures (left inferior parietal lobule, left

dorsal premotor cortex, and right hand/wrist motor representation), and between the right hand/wrist motor representation and the left posterior middle/inferior temporal gyrus, left medial fusiform gyrus, left dorsal occipital cortex, and left lateral occipital cortex (for t values, see Fig. 2a.ii; see also Table 2). In contrast, during tool picture matching, there were increases in functional connectivity among regions in the ventral stream (left posterior middle/inferior temporal gyrus, left medial fusiform gyrus), left dorsal occipital cortex, and left lateral occipital cortex (see Fig. 2a.ii and Table 2). The average Fisher-transformed correlation values, along with the distributions of individual participant results, associated with the interaction between Task and Epoch can be found in Fig. 2b. All of these patterns of functional connectivity were consistent when the global mean was regressed (see Supplemental Table 1).

Modulation of functional connectivity by tool pantomiming

Next, we sought to test the simple effect of Epoch separately for data from the tool pantomiming task and the tool picture matching task. Relative to the prestimulus condition, pantomiming tool use significantly increased functional connectivity among a number of tool-preferring regions (see Fig. 3a.i, red edges). Specifically, there were strong increases (1) among fronto-parietal motor structures (dorsal and ventral premotor cortex, the right hand/wrist motor representation, and the left inferior parietal lobule), (2) between the left inferior parietal lobule and the left posterior middle/inferior temporal gyrus, (3) and between the left posterior middle/inferior temporal gyrus, left lateral occipital cortex, and the primary motor representation of the right hand/wrist (see Fig. 3a.ii for

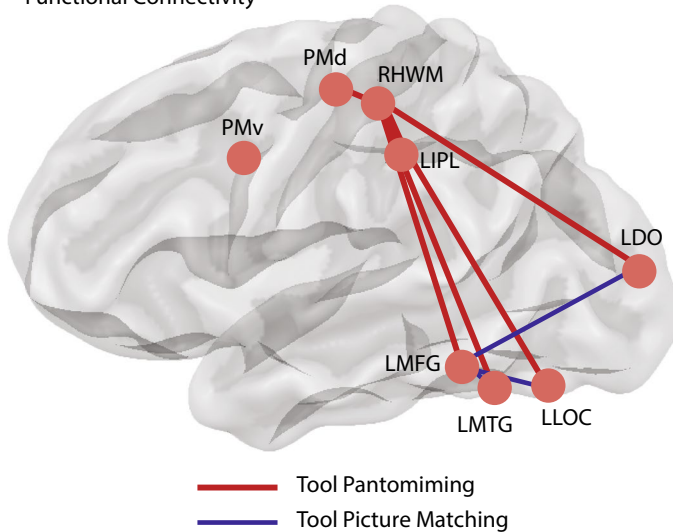
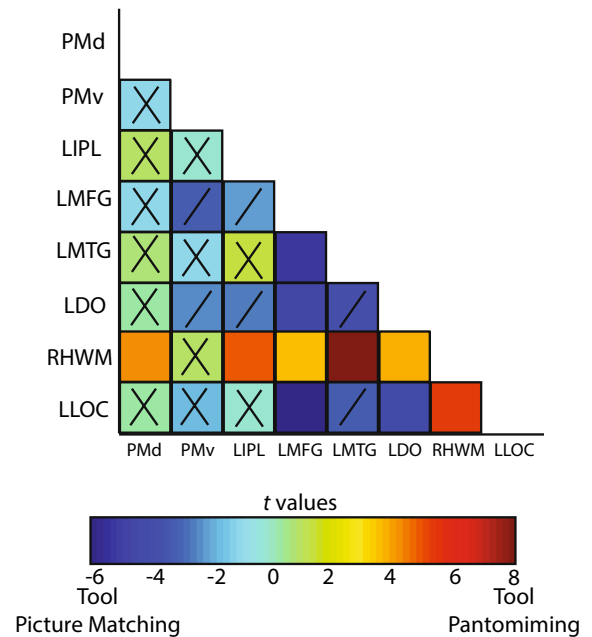
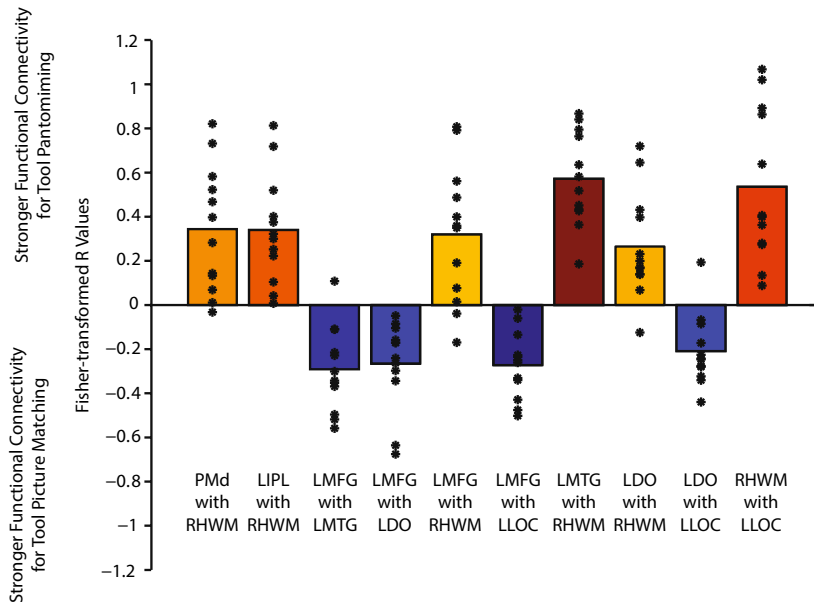
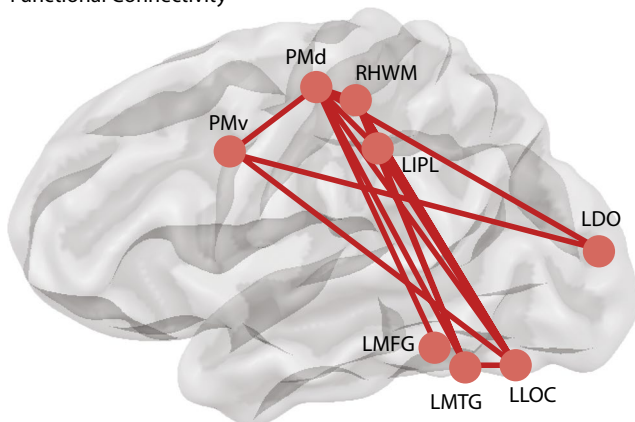
A Tool Pantomiming > Tool Picture Matching.A.i. ROI-based
Functional ConnectivityA.ii. *T*-values for the Interaction
Between Task and Epoch**B** Mean Correlation Coefficients and Participant Distributions for the Interaction between task (Tool Pantomiming and Tool Picture Matching) and epoch (stimulus driven versus prestimulus baseline).

Fig. 2 Interaction between epoch and task for functional connectivity for tool stimuli. **a** Red edges: relative to tool picture matching, tool pantomiming elicited increased functional connectivity among frontal–parietal ROIs and the left posterior middle/inferior temporal gyrus, left medial fusiform gyrus, left dorsal occipital cortex, and left lateral occipital cortex. Blue edges: tool picture matching elicited increased functional connectivity among left lateral occipital cortex, left posterior middle/inferior temporal gyrus, left medial fusiform gyrus, and left dorsal occipital cortex. The corresponding *t* values for

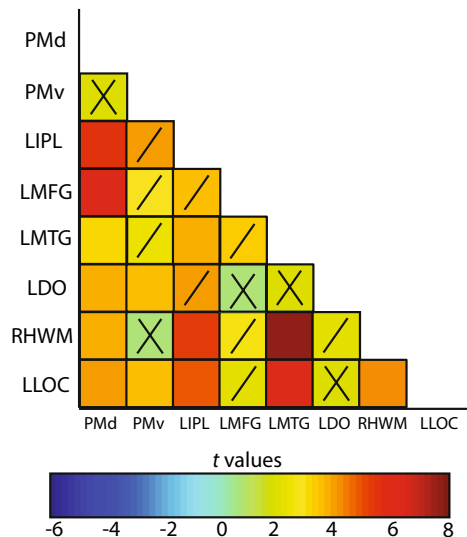
the interaction between epoch (stimulus on/off) and task are plotted as a heatmap in a.ii. Note that an ‘X’ in a cell in the heatmap corresponds to a non-significant *t* score associated with the interaction between Task and Epoch; a ‘/’ in a cell represents a *t* score that is significant but does not survive FDR-corrected alpha. **b** Average Fisher-transformed correlation coefficients and participant distributions are plotted for the edges that survive FDR-corrected alpha levels when using (1) all runs of data, (2) even runs, and (3) odd runs

A Tool Pantomiming > Pre-stimulus Functional Connectivity

A.i. ROI-based Functional Connectivity

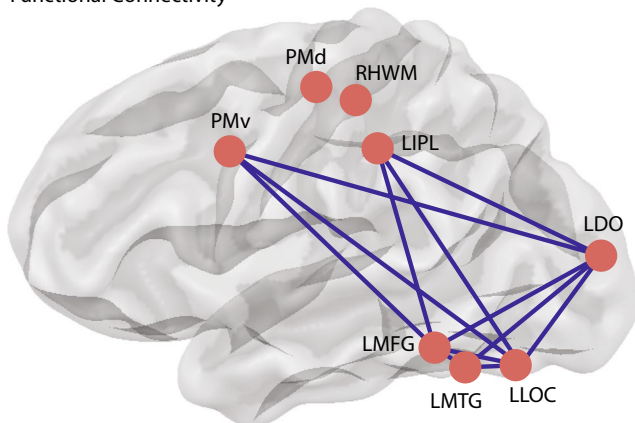


A.ii. *T*-values for the Contrast of Tool Pantomiming FC > Pre-Stimulus FC



B Tool Picture Matching > Pre-stimulus Functional Connectivity

B.i. ROI-based Functional Connectivity



B.ii. *T*-values for the Contrast of Tool Picture Matching FC > Pre-Stimulus FC

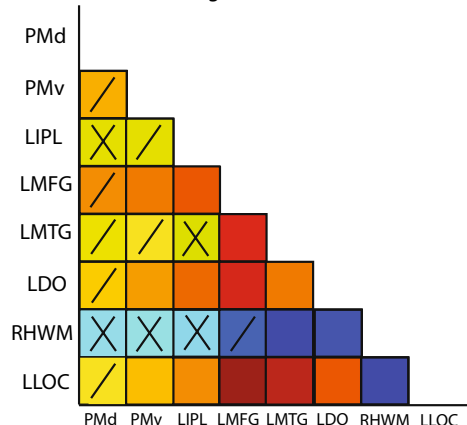


Fig. 3 Modulation of functional connectivity within task. **a** Relative to the prestimulus condition, tool pantomiming elicited increased functional connectivity among frontal–parietal structures (PMd, PMv, RHWM, and LIPL), left lateral occipital cortex, left dorsal occipital cortex, and ventral temporal tool areas (LMFG, LMTG; see a.i). In a.ii are the *t* values associated with the simple effects plotted as a heatmap. Note that an ‘X’ in a cell in the heatmap corresponds to a non-significant *t* score associated with the simple effect of Tool Pantomiming; a ‘/’ in a cell represents a *t* score that is significant but does not survive FDR-corrected alpha. **b** During tool picture matching, we observed increased functional connectivity, relative to the prestimulus condition, among left dorsal occipital cortex, left lateral

occipital cortex, ventral temporal tool areas (LMFG, LMTG), the left inferior parietal lobule, and the left ventral premotor cortex (see b.i). The *t* values associated with the simple effects are plotted as a heatmap in b.ii. Similar to the symbols in the heatmap of Fig. 3a.ii, an ‘X’ in a cell in the heatmap corresponds to a non-significant *t* score associated with the simple effect of Tool picture matching; a ‘/’ in a cell represents a *t* score that is significant but does not survive FDR-corrected alpha. *PMd* left dorsal premotor cortex, *PMv* left ventral premotor cortex, *RHWM* right hand/wrist motor, *LIPL* left inferior parietal lobule, *LMFG* left medial fusiform gyrus, *LMTG* left middle temporal gyrus

Table 3 *T* matrix for the contrast of stimulus-driven tool pantomiming > prestimulus tool pantomiming

	PMd	PMv	LIPL	LMFG	LMTG	LDO	RHWM	LLOC
PMd	–							
PMv	–	–						
LIPL	5.40	–	–					
LMFG	6.19	–	–	–				
LMTG	3.17	–	3.65	–	–			
LDO	3.80	3.53	–	–	–	–		
RHWM	3.81	–	5.26	–	7.61	–	–	
LLOC	4.01	3.50	4.78	–	6.01	–	4.22	–

Edges are reported that meet the criteria of surviving FDR $q < 0.05$ when the contrast was computed over all runs of data, and even and odd runs alone (split-half analysis). Positive t values indicate an increase in functional connectivity during pantomiming, while negative t values indicate an increase in functional connectivity during the prestimulus period

PMd left dorsal premotor cortex, *PMv* left ventral premotor cortex, *LIPL* left inferior parietal lobule, *LMFG* left medial fusiform gyrus, *LMTG* left posterior middle/inferior temporal gyrus, *LDO* left dorsal occipital cortex, *RHWM* right hand/wrist motor representation, *LLOC* left lateral occipital cortex

corresponding t values, and Table 3). All of these patterns of functional connectivity were consistent when the global mean was regressed (see Supplemental Table 2).

Modulation of functional connectivity by tool picture matching

There were increases associated with tool picture matching, compared to the prestimulus epochs, across a number of edges. Specifically: (1) the left lateral occipital cortex expressed increased functional connectivity with all regions of the Tool Processing Network except the right hand/wrist motor representation and the left dorsal premotor cortex; (2) the left medial fusiform gyrus exhibited increased functional connectivity with left ventral premotor cortex, the left inferior parietal lobule, and the left posterior middle/inferior temporal gyrus, and (3) the left dorsal occipital cortex

expressed an increase in functional connectivity with parietal and premotor structures, and with ventral stream structures (left medial fusiform gyrus and left posterior middle/inferior temporal gyrus), and left lateral occipital cortex (see Fig. 3b.i and Table 4). However, it should be noted that we observed increased functional connectivity between the left dorsal cortex and left lateral occipital cortex only when the global mean was regressed; the increase in functional connectivity between the left dorsal occipital cortex and the left posterior middle/inferior temporal gyrus was not observed when the global mean was regressed (see Supplemental Table 3).

Table 4 *T* matrix for the contrast of stimulus-driven tool picture matching > prestimulus tool picture matching

	PMd	PMv	LIPL	LMFG	LMTG	LDO	RHWM	LLOC
PMd	–							
PMv	–	–						
LIPL	–	–	–					
LMFG	–	4.36	4.93	–				
LMTG	–	–	–	6.28	–			
LDO	–	3.94	4.62	6.53	4.45	–		
RHWM	–	–	–	–	–	–	–	
LLOC	–	3.47	4.15	7.38	6.96	4.92	–	–

Edges are reported that meet the criteria of surviving FDR $q < 0.05$ when the contrast was computed over all runs of data, and even and odd runs alone (split-half analysis). Positive t values indicate an increase in functional connectivity during picture matching, while negative t values indicate an increase in functional connectivity during the prestimulus period

PMd left dorsal premotor cortex, *PMv* left ventral premotor cortex, *LIPL* left inferior parietal lobule, *LMFG* left medial fusiform gyrus, *LMTG* left posterior middle/inferior temporal gyrus, *LDO* left dorsal occipital cortex, *RHWM* right wrist motor representation, *LLOC* left lateral occipital cortex

Interaction between Task (pantomiming, picture matching) and Epoch (prestimulus, stimulus-driven) for animal stimuli

Control analyses evaluated whether the modulations (pantomiming versus picture matching) observed for tool stimuli are present for animal stimuli. We carried out parallel analyses with the pantomiming and picture matching data when animal stimuli were presented to participants. We first sought to measure which edges exhibited modulation in functional connectivity by Task (pantomiming > picture matching) and Epoch (stimulus-driven functional connectivity > prestimulus functional connectivity) for animal stimuli. There were no edges that survived FDR-corrected alpha levels, which indicates that task and epoch do not significantly modulate functional connectivity for any cued manual action; the lack of an effect for animal stimuli reduces the likelihood that the results observed for tool stimuli are due to general task demands (e.g., moving the hand in a stereotyped way in response to a visual stimulus). In addition, when using less strict alpha levels with animal stimuli (e.g., $p < 0.05$, uncorrected), we did not observe similar effects as those that were observed with tool stimuli, indicating that the lack of significant effects with animal stimuli was not due to adopting overly conservative statistical thresholds.

Modulation of functional connectivity by animal pantomiming

Consistent with the lack of an interaction between Task and Epoch for animal stimuli, there were no edges that survived FDR-corrected alpha levels ($q < 0.05$) in the animal pantomime petting task.

Modulation of functional connectivity by animal picture matching

There were no edges that survived FDR-corrected alpha levels ($q < 0.05$) in the picture matching task over animal stimuli.

Lack of an effect for animal stimuli is not because of reduced power

In the principal experiment, there were six tool stimuli and two animal stimuli with which each participant was presented in a run. Because there were not an equal number of animal stimuli as there were tool stimuli, it remains a possibility that the reason why the effects were not robust for animal stimuli, but were robust for tool stimuli, is simply because of this difference in power. This concern can be decisively addressed by computing functional connectivity as a function of task and epoch with only 2 tool stimuli per

run, iterating this analysis across every combination of 2 tool stimuli (6 items; 15 possible combinations). We carried out this analysis, and re-computed the interaction between task and epoch. We find that the results observed with 6 tools are present for the 2-tool analysis for the interaction of task and epoch (Supplemental Table 4), the simple effect of tool pantomiming compared to prestimulus epochs (Supplemental Table 5), and the simple effect of tool picture matching compared to prestimulus epochs (Supplemental Table 6). Note that again, edges were removed in 2-tool analyses if those edges did not meet the criteria of surviving FDR $q < 0.05$ in the full analysis and both split-half analysis (as described above).

Graph theoretic measures of functional connectivity in the tool processing network

Betweenness centrality during tool pantomiming and tool picture matching

During tool pantomiming, six vertices were identified as exhibiting “hub-like” properties (in descending order of centrality): the left dorsal premotor cortex, the left lateral occipital complex, the left posterior middle/inferior temporal gyrus, the left ventral premotor cortex, the left dorsal occipital cortex, the primary motor representation of the right hand/wrist, and the left inferior parietal lobule (see Fig. 4a). The increased centrality of those vertices during tool pantomiming was also supported by the edge centrality result, which indicated that edges among temporal regions and fronto-parietal structures were central to network connectivity during tool pantomiming (see Fig. 4a). Those edges were principally centered on the left inferior parietal lobule, dorsal premotor cortex, the primary motor representation of the right hand/wrist, left lateral occipital cortex, and the ventral stream (left medial fusiform gyrus, left posterior middle/inferior temporal gyrus; see Fig. 4a; for tool pantomime betweenness centrality, see Supplemental Table 7).

During tool picture matching, four vertices were identified as exhibiting “hub-like” properties (in descending order of centrality): the left lateral occipital cortex, the left medial fusiform gyrus, the left posterior middle/inferior temporal gyrus, and the left dorsal occipital cortex (see Fig. 4b). The edges most central to network function during tool picture matching were situated between: (1) left lateral occipital cortex and the ventral stream tool representations (left medial fusiform gyrus, left posterior middle/inferior temporal gyrus), (2) left lateral occipital cortex and fronto-parietal motor structures (left ventral premotor, left inferior parietal lobule), (3) the left medial fusiform and fronto-parietal motor structures, and (4) left dorsal occipital cortex and all other tool-preferring regions except dorsal premotor cortex (see Fig. 4b and Supplemental Table 8).

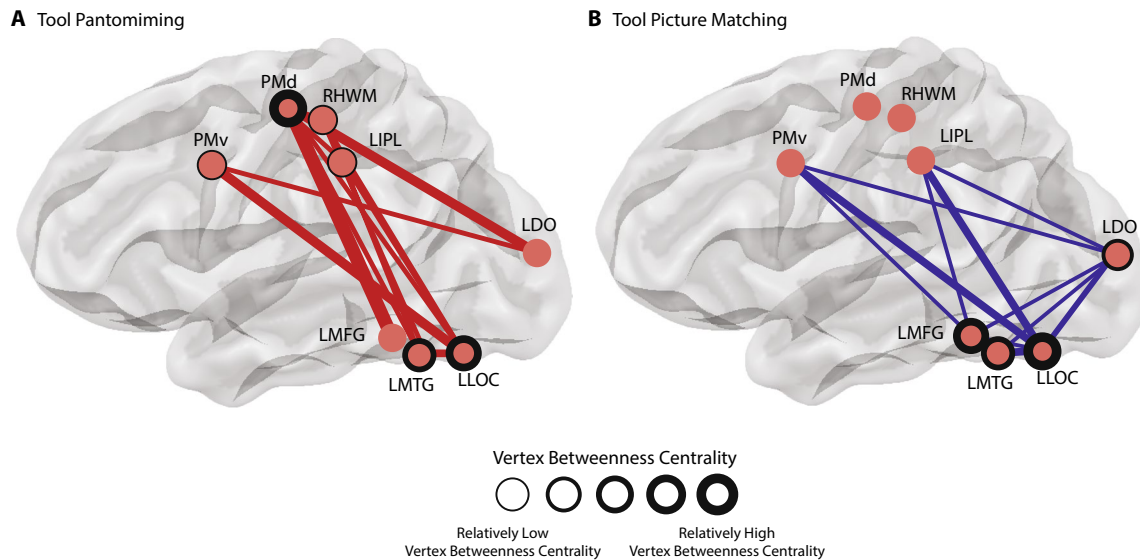


Fig. 4 Stimulus-driven betweenness centrality during tool pantomiming and tool picture matching. Edges and vertices were scaled by their betweenness centrality in the network. **a** Red edges: Increased betweenness centrality during pantomiming was observed for frontal–parietal areas and ventral stream regions [left lateral occipital cortex, and left ventral temporal tool areas (LMTG, LMFG)], and left dorsal occipital cortex. Black circles: the left dorsal premotor cortex, left lateral occipital cortex, and left posterior middle/inferior temporal gyrus were found to exhibit the most “hub-like” behavior during tool panto-

miming (i.e., high vertex centrality). **b** Blue edges: during tool picture matching the edges which exhibited increased centrality were situated in ventral temporal cortex (LMFG, LMTG), left lateral occipital cortex, the left dorsal occipital cortex. Black circles: The left lateral occipital cortex, left medial fusiform gyrus, left posterior/inferior middle temporal gyrus, and left dorsal occipital cortex were found to exhibit “hub-like” behavior during tool picture matching (i.e., high vertex centrality)

General discussion

We sought to address how functional interactions among a network of brain regions supporting processing of manipulable objects—the Tool Processing Network—are dynamically modulated in healthy adult participants. Participants performed an object pantomime and object picture matching task over the same visual input; a sparse design was employed that allowed us to probe how functional interactions across the Tool Processing Network are modulated during periods of active task (pantomime, picture matching) compared to periods just before a task epoch. There were strong increases in functional connectivity during tool pantomiming (compared to tool picture matching) between ventral stream regions and the left inferior parietal lobule, primary, and premotor cortex; in contrast, tool picture matching elicited increased functional connectivity among temporal lobe tool-preferring areas and left lateral occipital cortex. That pattern of dynamic modulation of functional connectivity as a function of task was not present when participants performed a pantomime or picture matching tasks over animal stimuli (pantomime petting, or picture matching). Analyses of edge and vertex betweenness centrality converged to indicate that pantomime of object use engaged a network integrating ventral and lateral temporal–occipital areas with frontal–parietal structures, while picture

matching led to higher connectivity within ventral and lateral temporal–occipital areas.

A recent fMRI study from Hutchison and Gallivan (2018) reported similar findings with respect to our results. In their experiment, participants were scanned in several different paradigms emphasizing motor processing (e.g., reaching-to-touch objects, reaching-to-grasp objects; e.g., see Gallivan et al. 2011, 2013) or visual/perceptual processing (e.g., attend to images of faces, tools, body parts; e.g., see Hutchison et al. 2014). Hutchison and Gallivan computed functional connectivity among fronto-parietal motor structures and ventral temporal tool areas, to measure the modulatory effect of task on functional connectivity between regions in the ventral and dorsal streams. They observed increased functional connectivity between left parietal tool representations and ventral–lateral occipitotemporal cortex during motor-based tasks that emphasized reaching-to-grasp objects. Thus, our results are consistent with their conclusion that regions in ventro-lateral occipitotemporal cortex may form a critical interface for dorsal–ventral stream interactions. In this regard, it is important to note that Hutchison and Gallivan computed functional connectivity over the time course from an entire functional run and different groups of participants completed the different experimental paradigms. The fact that there is such convergence between our reported findings and those of Hutchison and Gallivan

increase confidence in the pattern of findings across the two studies.

One important point of divergence between our findings and those of Hutchison and Gallivan (2018) is worth noting. We observed increased functional connectivity between the left inferior parietal lobule and ventro-lateral occipitotemporal cortex in both tool pantomiming and tool picture matching tasks (see Fig. 3). The design of our experiment was such that low-level visual stimulation was identical across pantomiming and picture matching tasks, and also identical across stimulus-driven and prestimulus epochs within a task. Thus any changes in functional connectivity were driven by the computations engaged by each stimulus in the context of the specific task, over and above the actual images used in the experiment. We believe that these differences in our design may explain why we observed parietal-to-temporal/occipital connectivity during object picture matching, while Hutchison and Gallivan did not. It will be important to further pursue these effects using experimental approaches in which (1) all effects are computed within participant on individual subject-defined ROIs, (2) perceptual variables are held constant across tasks, and (3) low-level perceptual stimulation is held constant across a run, so that such low-level variables do not correlate with task performance.

One generalization that emerges from our findings, across the functional connectivity and betweenness centrality analyses, is that there are robust interactions between left lateral occipital cortex and the Tool Processing Network. Lateral occipital cortex is critical for representing the visual form and structure of objects (e.g., Goodale et al. 1991), perhaps, in a part-based manner (Hayworth et al. 2011; see also; Hayworth and Biederman 2006), and may play a role in multisensory integration of visual and haptic information (e.g., Amedi et al. 2001; Erdogan et al. 2016; Yalachkov et al. 2015; but see Snow et al. 2015). However, there are no clear tool preferences in lateral occipital cortex, at least at the topographic granularity afforded by fMRI. In a slightly more anterior region, in the left occipitotemporal cortex, Bracci et al. (2012) reported overlap between regions that exhibited increased BOLD contrast for hands and tools; interestingly, there was no overlap with extrastriate regions that process whole bodies. It should be noted that the functionally defined left posterior middle/inferior temporal gyrus in the current study may be anterior (based on Talairach coordinates) to the area of overlap for hands and tools, as reported by Bracci et al. (2012) (see also Bracci and Peelen 2013; Bracci and Op de Beeck 2016). Bracci et al. (2012) also found that tool- and hand-preferring regions in lateral occipitotemporal cortex expressed privileged functional connectivity to parietal regions involved in praxis.

Taking a step back, our findings indicate dynamic interactions among regions that process object form and motor-relevant information during pantomiming, and

among regions in ventral and lateral temporal cortex that support high-level visual and semantic analysis during picture matching. To access object-directed manipulation information, it is important to extract object form and surface properties (e.g., texture) along with other properties processed in the ventral stream (e.g., object weight; e.g., see Gallivan et al. 2014), and to bring those visual and material properties into alignment with visuomotor and praxis representations in frontal–parietal structures. It is particularly relevant to note here that while participants were cued to pantomime by images of objects, the actions that participants performed were not directed at those objects. Thus, object pantomime (even to visual presentation of objects) is not a ‘visuomotor’ task in the sense of the types of visuomotor tasks that are known to be propagated differentially through dorsal stream pathways (e.g., Goodale et al. 1991). This also represents an important difference between our study and that of Hutchison and Gallivan (2018) in which participants were performing object-directed reaches and grasps (see discussion in Goodale and Milner 1992; Goodale et al. 1994).

Prior research with neuropsychological patients indicates that complex object-associated manipulation information is processed by the left inferior parietal lobule, and specifically the supramarginal gyrus (e.g., Buxbaum et al. 2000; Mahon et al. 2007; Negri et al. 2007; Garcea et al. 2013; for review, see Johnson-Frey 2004; Mahon and Caramazza 2005). Subsequent neuroimaging work confirms a key role for the supramarginal gyrus in representing complex object-directed manipulation (Kellenbach et al. 2003; Rumiati et al. 2004; Boronat et al. 2005; Mahon et al. 2007; Canessa et al. 2008; Chen et al. 2016, 2017b). We have previously argued that access to manipulation knowledge from visual input is contingent on retrieval of object identity in the ventral stream (e.g., see Almeida et al. 2013; Garcea et al. 2016; Kristensen et al. 2016; Mahon et al. 2013; see also; Binkofski and Buxbaum 2013). Consistent with that argument, here, we observed consistent increases in task-based functional connectivity between the left inferior parietal lobule and the ventral stream across both tool pantomiming and picture matching tasks (see Fig. 3a, b).

Patient evidence consistent with the hypothesis that accessing object-directed manipulation and functionally appropriate object grasps is contingent on analysis by the ventral stream is also provided by the work of Carey, Harvey and Milner (1996). Those authors tested the visuomotor abilities of patient DF, a visual object agnostic, in an object grasping and object use task. Carey and colleagues showed that DF was able to grasp objects in a way that respected the objects’ volumetric and spatial properties (i.e., orientation and shape). However, DF failed to generate a functionally appropriate grasp on the basis of visual input (e.g., she was as likely to grasp a fork by the tines as by the handle). Thus,

the ability to generate a functionally appropriate grasp that anticipates the way in which the object will be manipulated was impaired by the bilateral lateral occipital cortex lesions in DF. Our functional connectivity results are entirely consistent with those neuropsychological data, and provide another level of anatomical detail on functional interactions between ventral stream and frontal–parietal motor-relevant structures.

Our results also interact with the issue of whether tool pantomiming is supported by perceptual representations in the ventral stream. A classic demonstration of the dissociation between actions guided by visual input versus actions guided by perceptual representations of visual input is provided by the study of Goodale et al. (1994). Goodale and colleagues presented the visual agnostic patient DF with a small graspable target 20 cm from a starting point; in one condition, she was cued to grasp the object immediately; while in another condition, there was a 2-s delay between the presentation of the object and the initiation of her action. Furthermore, in the 2-s delay condition, the object was removed, forcing DF to use perceptual representations of the object to guide her visuomotor behavior. In the no-delay condition, DF scaled her grip aperture in a way that reflected the size of the to-be grasped object, as had been demonstrated by prior studies from the same group with this patient (e.g., Goodale et al. 1991). However, in the 2-s delay condition, DF did not accurately scale her grip aperture to the object, presumably because perceptual representations of the object were needed to support grip scaling in the absence of the object, which was compromised by her bilateral LOC lesions. These and other findings (e.g., Carey et al. 1996) suggest that parietal-to-temporal functional connectivity must be key for integrating object knowledge in the ventral stream with action processes in parietal cortex, and especially in situations in which perceptual representations are used to drive actions. It is possible, perhaps likely, that the experimental paradigm of ‘pantomiming’ object use may engage perceptual representations in the ventral stream more so than would actual object use. This is an important issue, because ‘pantomiming’ object use is a widely used test to establish the presence of apraxia; thus, it may be that some variants of apraxia reflect deregulation or disturbance of connectivity between ventral stream perceptual representations and praxis representations in parietal cortex, rather than disruption of the praxis representations themselves (e.g., see Martin et al. 2017).

An important goal for future research will be to understand the real-time dynamics of functional interactions among regions in the Tool Processing Network when participants are using real tools and when pantomiming object use (e.g., see Brandi et al. 2014; see also; Freud et al. 2018; Snow et al. 2011). Because participants did not receive visual feedback of their hand actions during object pantomiming

in the current study, mental imagery processes may have been overly engaged during the pantomime task. Future work in which participants can reach for and manipulate objects, while receiving visual feedback would be crucial for understanding how ventral stream perceptual representations interact with dorsal stream processes, and how dorsal stream perceptual processes interact with visually guided actions (for relevant findings, see Cavina-Pratesi et al. 2010; Culham et al. 2003; Freud et al. 2017a, b, 2018; Gallivan et al. 2013, 2015). Similarly, future work using methods with high temporal resolution (magnetoencephalography, electroencephalography, electrocorticography; e.g., see Caruana et al. 2017) would permit fine-grained analysis of real-time changes in functional coupling among regions of the Tool Processing Network during actual tool use.

Acknowledgements This research was supported by NIH Grant R01 NS089069 and NSF Grant BCS-1349042 to BZM, and by a University of Rochester Center for Visual Science predoctoral training fellowship (NIH training Grant 5T32EY007125-24) to FEG. Preparation of the ms was supported, in part, by a Moss Rehabilitation Research Institute postdoctoral training fellowship (NIH 5T32HD071844-05) to F.E.G. RV was supported by an NSF Research Experiences for Undergraduates Grant to DAN at the Rochester Institute of Technology (1358583); DAN was also supported by NSF Grant 1019532.

References

- Almeida J, Fintzi AR, Mahon BZ (2013) Tool manipulation knowledge is retrieved by way of the ventral visual object processing pathway. *Cortex* 49:2334–2344
- Amedi A, Malach R, Hendler T, Peled S, Zohary E (2001) Visuo-haptic object-related activation in the ventral visual pathway. *Nat Neurosci* 4(3):324–330
- Beauchamp MS, Lee KE, Haxby JV, Martin A (2002) Parallel visual motion processing streams for manipulable objects and human movements. *Neuron* 34:149–159
- Beauchamp MS, Lee KE, Haxby JV, Martin A (2003) fMRI responses to video and point-light displays of moving humans and manipulable objects. *J Cogn Neurosci* 15:991–1001
- Bedny M, Caramazza A (2011) Perception, action, and word meanings in the human brain: the case from action verbs. *Ann N Y Acad Sci* 1224(1):81–95
- Bedny M, Caramazza A, Grossman E, Pascual-Leone A, Saxe R (2008) Concepts are more than percepts: the case of action verbs. *J Neurosci* 28(44):11347–11353
- Bedny M, Caramazza A, Pascual-Leone A, Saxe R (2012) Typical neural representations of action verbs develop without vision. *Cereb Cortex* 22(2):286–293
- Binkofski F, Buxbaum LJ (2013) Two action systems in the human brain. *Brain Lang* 127(2):222–229
- Binkofski F, Dohle C, Posse S, Stephan KM, Hefter H, Seitz RJ, Freund HJ (1998) Human anterior intraparietal area subserves prehension A combined lesion and functional MRI activation study. *Neurology* 50(5):1253–1259
- Boronat CB, Buxbaum LJ, Coslett HB, Tang K, Saffran EM, Kimberg DY, Detre JA (2005) Distinctions between manipulation and function knowledge of objects: evidence from functional magnetic resonance imaging. *Cogn Brain Res* 23(2):361–373

- Bracci S, Op de Beeck H (2016) Dissociations and associations between shape and category representations in the two visual pathways. *J Neurosci* 36(2):432–444
- Bracci S, Peelen MV (2013) Body and object effectors: the organization of object representations in high-level visual cortex reflects body–object interactions. *J Neurosci* 33(46):18247–18258
- Bracci S, Cavina-Pratesi C, Ietswaart M, Caramazza A, Peelen MV (2012) Closely overlapping responses to tools and hands in left lateral occipitotemporal cortex. *J Neurophysiol* 107(5):1443–1456
- Brandes U, Borgatti SP, Freeman LC (2015) Maintaining the duality of closeness and betweenness centrality social networks. *Soc Netw* 44:153–159
- Brandi ML, Wohlschläger A, Sorg C, Hermsdörfer J (2014) The neural correlates of planning and executing actual tool use. *J Neurosci* 34(39):13183–13194
- Bruffaerts R, De Weer AS, De Grauwe S, Thys M, Dries E, Thijs M et al (2014) Noun and knowledge retrieval for biological and non-biological entities following right occipitotemporal lesions. *Neuropsychologia* 62:163–174
- Buxbaum LJ (2017) Learning, remembering, and predicting how to use tools: distributed neurocognitive mechanisms: comment on Osiurak and Badets (2016). *Psychol Rev* 124:346–360
- Buxbaum LJ, Veramonti T, Schwartz MF (2000) Function and manipulation tool knowledge in apraxia: knowing “what for” but not “how”. *Neurocase* 6:83–97
- Buxbaum LJ, Shapiro AD, Coslett HB (2014) Critical brain regions for tool-related and imitative actions: a componential analysis. *Brain* 137:1971–1985
- Canessa N, Borgo F, Cappa SF, Perani D, Falini A, Buccino G, Shallice T (2008) The different neural correlates of action and functional knowledge in semantic memory: an fMRI study. *Cereb Cortex* 18(4):740–751
- Cant JS, Goodale MA (2007) Attention to form or surface properties modulates different regions of human occipitotemporal cortex. *Cereb Cortex* 17:713–731
- Cant JS, Goodale MA (2011) Scratching beneath the surface: New insights into the functional properties of the lateral occipital area and parahippocampal place area. *J Neurosci* 31:8248–8258
- Carey DP, Harvey M, Milner AD (1996) Visuomotor sensitivity for shape and orientation in a patient with visual form agnosia. *Neuropsychologia* 34:329–337
- Caruana F, Avanzini P, Mai R, Pelliccia V, LoRusso G, Rizzolatti, Orban GA (2017) Decomposing tool-action observation: a stereo-EEG study. *Cereb Cortex* 27(8):4229–4243
- Cavina-Pratesi C, Goodale MA, Culham JC (2007) fMRI reveals a dissociation between grasping and perceiving the size of real 3D objects. *PLoS One* 2:1–14
- Cavina-Pratesi C, Kentridge RW, Heywood CA, Milner AD (2009) Separate processing of texture and form in the ventral stream: evidence from fMRI and visual agnosia. *Cereb Cortex* 20(2):433–446
- Cavina-Pratesi C, Monaco C, Fattori P, Galletti C, McAdam TD, Quinlan DJ et al (2010) Functional magnetic resonance imaging reveals the neural substrates of arm transport and grip formation in reach-to-grasp actions in humans. *J Neurosci* 30:10306–10323
- Chao LL, Martin A (2000) Representation of manipulable man-made objects in the dorsal stream. *Neuroimage* 12:478–484
- Chao LL, Haxby JV, Martin A (1999) Attribute-based neural substrates in temporal cortex for perceiving and knowing about objects. *Nat Neurosci* 2:913–919
- Chen Q, Garcea FE, Mahon BZ (2016) The representation of object-directed action and function knowledge in the human brain. *Cereb Cortex* 26:1609–1618
- Chen Q, Garcea FE, Almeida J, Mahon BZ (2017a) Connectivity-based constraints on category-specificity in the ventral object processing pathway. *Neuropsychologia* 105:184–196
- Chen Q, Garcea FE, Jacobs R, Mahon BZ (2017b) Abstract representations of object directed action in the left inferior parietal lobule. *Cereb Cortex*, 1–13. <https://doi.org/10.1093/cercor/bhx120>
- Cubelli R, Marchetti C, Boscolo G, Della Salla S (2000) Cognition in action: testing a model of limb apraxia. *Brain Cogn* 44:144–165
- Culham JC, Danckert SL, DeSouza JFX, Gati JS et al (2003) Visually guided grasping produces fMRI activation in dorsal but not ventral stream brain areas. *Exp Brain Res* 153:180–189
- Eklund A, Nichols TE, Knutsson H (2016) Cluster failure: why fMRI inferences for spatial extent have inflated false-positive rates. *Proc Natl Acad Sci* 113(28):7900–7905
- Erdogan G, Chen Q, Garcea FE, Mahon BZ, Jacobs RA (2016) Multisensory part-based representations of objects in human lateral occipital cortex. *J Cogn Neurosci* 28(6):869–881
- Fang F, He S (2005) Cortical responses to invisible objects in the human dorsal and ventral pathways. *Nat Neurosci* 8:1380–1385
- Fintzi AR, Mahon BZ (2014) A bimodal tuning curve for spatial frequency across left and right human orbital frontal cortex during object recognition. *Cereb Cortex* 24:1311–1318
- Freeman LC (1977) A set of measures of centrality based on betweenness. *Sociometry* 40:35–41
- Freeman LC, Borgatti SP, White DR (1991) Centrality in valued graphs: a measure of betweenness based on network flow. *Soc Netw* 13(2):141–154
- Freud E, Plaut DC, Behrmann M (2016) ‘What’ is happening in the dorsal visual pathway. *Trends Cogn Sci* 20(10):773–784
- Freud E, Culham JC, Plaut DC, Behrmann M (2017a) The large-scale organization of shape processing in the ventral and dorsal pathways. *eLife* 6:1–26
- Freud E, Ganel T, Shelef I, Hammer MD, Avidan G, Behrmann M (2017b) Three-dimensional representations of objects in dorsal cortex are dissociable from those in ventral cortex. *Cereb Cortex* 27(1):422–434
- Freud E, Macdonald SN, Chen J, Quinlan DJ, Goodale MA, Culham JC (2018) Getting a grip on reality: grasping movements directed to real objects and images rely on dissociable neural representations. *Cortex* 98:34–48
- Frey SH, Vinton D, Norlund R, Grafton ST (2005) Cortical topography of human anterior intraparietal cortex active during visually guided grasping. *Cogn Brain Res* 23(2):397–405
- Galletti C, Battaglini PP, Fattori P (1993) Parietal neurons encoding spatial locations in craniotopic coordinates. *Exp Brain Res* 96:221–229
- Gallivan JP, McLean DA, Smith FW, Culham JC (2011) Decoding effector-dependent and effector independent movement intentions from human parieto-frontal brain activity. *J Neurosci* 31:17149–17168
- Gallivan JP, McLean DA, Valyear KF, Culham JC (2013) Decoding the neural mechanisms of human tool use. *eLife* 2:1–29
- Gallivan JP, Cant JS, Goodale MA, Flanagan JR (2014) Representation of object weight in the human ventral visual cortex. *Curr Biol* 24:1–8
- Gallivan JP, Johnsrude IS, Flanagan JR (2016) Planning ahead: object-directed sequential actions decoded from human frontoparietal and occipitotemporal networks. *Cereb Cortex* 26(2):708–730
- Garcea FE, Mahon BZ (2014) Parcellation of left parietal tool representations by functional connectivity. *Neuropsychologia* 60:131–143
- Garcea FE, Dombovy M, Mahon BZ (2013) Preserved tool knowledge in the context of impaired action knowledge: implications for models of semantic memory. *Front Hum Neurosci* 7:1–18

- Garcea FE, Kristensen S, Almeida J, Mahon BZ (2016) Resilience to the contralateral visual field bias as a window into object representations. *Cortex* 81:14–23
- Garcea FE, Chernoff BL, Diamond B, Lewis W, Sims MH, Tomlinson SB, Mahon BZ (2017) Direct electrical stimulation in the human brain disrupts melody processing. *Curr Biol* 27(17):2684–2691
- Gleich DF (2006). <https://www.mathworks.com/matlabcentral/fileexchange/10922-matlabbg1>. Accessed 21 Mar 2016
- Goldenberg G (2009) Apraxia and the parietal lobes. *Neuropsychologia* 47:1449–1459
- Goodale MA, Milner AD (1992) Separate visual pathways for perception and action. *Trends Neurosci* 15:20–25
- Goodale MA, Milner AD, Jakobson LS, Carey DP (1991) A neurological dissociation between perceiving objects and grasping them. *Nature* 349:154–156
- Goodale MA, Jakobson LS, Keillor JM (1994) Differences in the visual control of pantomimed and natural grasping movements. *Neuropsychologia* 32(10):1159–1178
- Gotts SJ, Saad ZS, Jo HJ, Wallace GL, Cox RW et al (2013a) The perils of global signal regression for group comparisons: a case study of Autism Spectrum Disorders. *Front Hum Neurosci* 7:1–20
- Gotts SJ, Jo HJ, Wallace GL, Saad ZS, Cox RW, Martin A (2013b) Two distinct forms of functional lateralization in the human brain. *Proc Natl Acad Sci* 110(36):E3435–E3444
- Grafton ST, Fadiga L, Arbib MA, Rizzolatti G (1997) Premotor cortex activation during observation of familiar tools. *NeuroImage* 6:231–236
- Grill-Spector K, Kushnir T, Hendler T, Edelman S, Itzhak Y, Malach R (1998) A sequence of object-processing stages revealed by fMRI in the human occipital lobe. *Hum Brain Mapp* 6(4):316–328
- Hayworth KJ, Biederman I (2006) Neural evidence for intermediate representations in object recognition. *Vis Res* 46(23):4024–4031
- Hayworth KJ, Lescroart MD, Biederman I (2011) Neural encoding of relative position. *J Exp Psychol Hum Percept Perform* 37:1032–1050
- Hutchison RM, Gallivan JP (2018) Functional coupling between frontoparietal and occipitotemporal pathways during action and perception. *Cortex* 98:8–27
- Hutchison RM, Culham JC, Everling S, Flanagan JR, Gallivan JP (2014) Distinct and distributed functional connectivity patterns across cortex reflect the domain-specific constraints of object, face, scene, body, and tool category-selective modules in the ventral visual pathway. *Neuroimage* 96:216–236
- Ishibashi R, Pobric G, Saito S, Lambon Ralph MA (2016) The neural network for tool-related cognition: an activation likelihood estimation meta-analysis of 70 neuroimaging contrasts. *Cogn Neuropsychol* 33(3–4):241–256
- Johnson-Frey S (2004) The neural bases of complex tool use in humans. *Trends Cogn Sci* 8:71–78
- Kable JW, Lease-Spellmeyer J, Chatterjee A (2002) Neural substrates of action event knowledge. *J Cogn Neurosci* 14(5):795–805
- Kastner S, Chen Q, Jeong SK, Mruczek REB (2017) A brief comparative review of primate posterior parietal cortex: a novel hypothesis on the human toolmaker. *Neuropsychologia* 105:123–134
- Kellenbach M, Brett M, Patterson K (2003) Actions speak louder than functions: the importance of manipulability and action in tool representation. *Cogn Neurosci* 15(1):30–46
- Kemmerer D, Castillo JG, Talavage T, Patterson S, Wiley C (2008) Neuroanatomical distribution of five semantic components of verbs: evidence from fMRI. *Brain Lang* 107(1):16–43
- Konen CS, Kastner S (2008) Two hierarchically organized neural systems for object information in human visual cortex. *Nat Neurosci* 11(2):224
- Konen CS, Mruczek REB, Montoya JL, Kastner S (2013) Functional organization of human posterior parietal cortex: grasping- and reaching-related activations relative to topographically organized cortex. *J Neurophysiol* 109:2897–1908
- Kristensen S, Garcea FE, Mahon BZ, Almeida J (2016) Temporal frequency tuning reveals interactions between the dorsal and ventral visual streams. *J Cogn Neurosci* 28:1295–1302
- Lewis J (2006) Cortical networks related to human use of tools. *Neuroscientist* 12:211–231
- Liepmann H (1905) The left hemisphere and action. (Translation from Munch. Med. Wschr. 48–49). (Translations from Liepmann's essays on apraxia. In Research Bulletin (vol 506). Department of Psychology, University of Western Ontario, London, Ont.; 1980)
- Mahon BZ, Caramazza A (2005) The orchestration of the sensory-motor systems: clues from neuropsychology. *Cogn Neuropsychol* 22:480–494
- Mahon BZ, Milleville S, Negri GAL, Rumiati RI et al (2007) Action-related properties of objects shape object representations in the ventral stream. *Neuron* 55:507–520
- Mahon BZ, Kumar N, Almeida J (2013) Spatial frequency tuning reveals interactions between the dorsal and ventral visual systems. *J Cogn Neurosci* 25:862–871
- Malach R, Reppas JB, Benson RR, Kwong KK, Jiang H, Kennedy WA, Tootell RB (1995) Object-related activity revealed by functional magnetic resonance imaging in human occipital cortex. *Proc Natl Acad Sci* 92(18):8135–8139
- Martin A (2007) The representation of object concepts in the brain. *Annu Rev Psychol* 58:25–45
- Martin M, Dressing A, Bormann T, Schmidt CS, Kümmerer D, Beume L, Weiller C (2017) Componential network for the recognition of tool-associated actions: evidence from voxel-based lesion-symptom mapping in acute stroke patients. *Cereb Cortex* 27:4139–4152
- Miceli G, Fouch E, Capasso R, Shelton JR, Tomaiuolo F, Caramazza A (2001) The dissociation of color from form and function knowledge. *Nat Neurosci* 4:662–667
- Milner AD, Goodale MA (2008) Two visual systems re-viewed. *Neuropsychologia* 46(3):774–785
- Moll J, de Oliveira-Souza R, Passman LJ, Cunha FC, Souza-Lima F, Andreiuolo PA (2000) Functional MRI correlates of real and imagined tool-use pantomimes. *Neurology* 54(6):1331–1336
- Negri GAL, Rumiati RI, Zadini A, Ukmir M, Mahon BZ, Caramazza A (2007) What is the role of motor simulation in action and object recognition? Evidence from apraxia. *Cogn Neuropsychol* 24:795–816
- Noppeney U, Price CJ, Penny WD, Friston KJ (2006) Two distinct neural mechanisms for category-selective responses. *Cereb Cortex* 16:437–445
- Ochipa C, Rothi LJG, Heilman KM (1989) Ideational apraxia: a deficit in tool selection and use. *Ann Neurol* 25:190–193
- Orban GA, Caruana F (2014) The neural basis of human tool use. *Front Psychol* 5:1–12
- Peelen MV, Romagno D, Caramazza A (2012) Independent representations of verbs and actions in left lateral temporal cortex. *J Cogn Neurosci* 24(10):2096–2107
- Peelen MV, Bracci S, Lu X, He C, Caramazza A, Bi Y (2013) Tool selectivity in left occipitotemporal cortex develops without vision. *J Cogn Neurosci* 25(8):1225–1234
- Peeters RR, Rizzolatti G, Orban GA (2013) Functional properties of the left parietal tool use region. *Neuroimage* 78:83–93
- Pelli DG (1997) The VideoToolbox software for visual psychophysics: transforming numbers into movies. *Spat Vis* 10:377–401
- Pisella L, Grea H, Tilikete C, Vighetto A, Desmurget M, Rode G, Rossetti Y (2000) An 'automatic pilot' for the hand in human

- posterior parietal cortex: toward reinterpreting optic ataxia. *Nat Neurosci* 3(7):729–736
- Pisella L, Binkofski F, Lasek K, Toni I, Rossetti Y (2006) No double-dissociation between optic ataxia and visual agnosia: multiple sub-streams for multiple visuo-manual integrations. *Neuropsychologia* 44(13):2734–2748
- Rossetti Y, Pisella L, Vighetto A (2003) Optic ataxia revisited. *Exp Brain Res* 153(2):171–179
- Rothi LJG, Ochipa C, Heilman KM (1991) A cognitive neuropsychological model of limb praxis. *Cogn Neuropsychol* 8:443–458
- Rubinov M, Sporns O (2010) Complex network measures of brain connectivity: uses and interpretations. *NeuroImage* 52:1059–1069
- Rumiati RI, Weiss PH, Shallice T, Ottoboni G, Noth J, Zilles K, Fink GR (2004) Neural basis of pantomiming the use of visually presented objects. *Neuroimage* 21(4):1224–1231
- Saad ZS, Reynolds RC, Jo HJ, Gotts SJ, Chen G et al (2013) Correcting brain-wide correlation differences in resting-state fMRI. *Brain Connect* 3:339–352
- Salazar-López E, Schwaiger BJ, Hermsdörfer J (2016) Lesion correlates of impairments in actual tool use following unilateral brain damage. *Neuropsychologia* 84:167–180
- Schwarzbach J (2011) A simple framework (ASF) for behavioral and neuroimaging experiments based on psychophysics toolbox for MATLAB. *Behav Res* 43:1194–1201
- Simmons WK, Ramjee V, Beauchamp MS, McRae K, Martin A, Barsalou LW (2007) A common neural substrate for perceiving and knowing about color. *Neuropsychologia* 45(12):2802–2810
- Snow JC, Pettypiece CE, McAdam TD, McLean AD, Stroman PW, Goodale MA, Culham JC (2011) Bringing the real world into the fMRI scanner: repetition effects for pictures versus real objects. *Sci Rep* 1:1–10, Article no. 130
- Snow JC, Goodale MA, Culham JC (2015) Preserved haptic shape processing after bilateral LOC lesions. *J Neurosci* 35(40):13745–13760
- Stasenka A, Garcea FE, Dombrov M, Mahon BZ (2014) When concepts lose their color: a case of object-color knowledge impairment. *Cortex* 58:217–238
- Stevens WD, Tessler MH, Peng CS, Martin A (2015) Functional connectivity constrains the category-related organization of human ventral occipitotemporal cortex. *Hum Brain Mapp* 36(6):2187–2206
- Talairach J, Tournoux P (1988) Co-planar stereotaxic atlas of the human brain. 3-Dimensional proportional system: an approach to cerebral imaging. Thieme Medical Publishers, New York
- Tranel D, Damasio H, Damasio AR (1997) A neural basis for the retrieval of conceptual knowledge. *Neuropsychologia* 35(10):1319–1327
- Tranel D et al (2003) Neural correlates of conceptual knowledge for actions. *Cogn Neuropsychol* 20:409–432
- Valyear KF, Cavina-Pratesi C, Stiglick AJ, Culham JC (2007) Does tool-related fMRI activity within the intraparietal sulcus reflect the plan to grasp? *Neuroimage* 36:T94–T108
- Van Dromme IC, Premereur E, Verhoef BE, Vanduffel W, Janssen P (2016) Posterior parietal cortex drives inferotemporal activations during three-dimensional object vision. *PLoS Biol* 14(4):e1002445
- Vingerhoets G, Clauwaert A (2015) Functional connectivity associated with hand shape generation: Imitating novel hand postures and pantomiming tool grips challenge different nodes of a shared neural network. *Hum Brain Mapp* 36(9):3426–3440
- Yalachkov Y, Kaiser J, Doehrmann O, Naumer MJ (2015) Enhanced visuo-haptic integration for the non-dominant hand. *Brain Res* 1614:75–85